

HUBBLE SPACE TELESCOPE OBSERVATIONS OF THE CRAB NEBULA

J. Jeff Hester

Department of Physics and Astronomy, Arizona State University, Box 871504, Tempe AZ 85287-1504, USA;
jjh@cygloop.la.asu.edu

RESUMEN

La Nebulosa del Cangrejo es uno de los objetos mejor estudiados en el cielo. A pesar de esto, las observaciones de alta resolución espacial en el Cangrejo, usando el *Telescopio Espacial Hubble* nos han llevado a nuevos descubrimientos acerca del Cangrejo que además de aclarar nuestra comprensión del objeto han hecho surgir nuevas preguntas. Entre los puntos sobresalientes acerca de la nebulosa sincrotrónica están la definición de la estructura axisimétrica de la nebulosa sincrotrónica, incluyendo la identificación de nuevos rasgos tanto en el viento ecuatorial como en los dos chorros polares del pulsar. Estos incluyen el descubrimiento de un nudo brillante de emisión sincrotrónica a $0'.5$ del pulsar, localizado a lo largo del eje del sistema. Un programa de monitoreo temporal muestra que el interior del Cangrejo es mucho más dinámico que lo que previamente se había aceptado. Se han visto rasgos que se alejan del pulsar a velocidades del orden de $0.5c$ y que cambian su apariencia dramáticamente en periodos del orden de una semana. Observaciones de esas eyecciones filamentosas en el Cangrejo, muestran que los filamentos son el resultado de inestabilidades Rayleigh-Taylor en la interfase entre la nebulosa sincrotrónica y la eyección barrida. El hecho de que la nebulosa sincrotrónica no ha salido del confinamiento de los filamentos, puede ser mejor entendida si hay un remanente extendido de eyección en expansión libre rodeando al Cangrejo. La interfase inestable R-T puede ser entendida cuantitativamente como la región de enfriamiento, detrás de un choque impulsado sobre el remanente por la presión de la nebulosa sincrotrónica.

ABSTRACT

The Crab Nebula is one of the best studied objects in the sky. Despite this fact, high spatial resolution observations of the Crab using the *Hubble Space Telescope* have lead to a number of new discoveries about the Crab that have both clarified our understanding, and raised new questions. Highlights of the work on the synchrotron nebula include clarification of the axisymmetrical structure of the inner synchrotron nebula, including identification of new features in both the equatorial wind and two polar jets from the pulsar. These include discovery of a bright knot of synchrotron emission only $0'.5$ from the pulsar, located along the axis of the system. A program of temporal monitoring shows that the inner Crab is far more dynamical than previously understood. Features are seen moving away from the pulsar at speeds of order $0.5c$, and changing their appearance dramatically over periods of order one week. Observations of the filamentary ejecta in the Crab show that the filaments are the result of Rayleigh-Taylor instabilities in the interface between the synchrotron nebula and swept-up ejecta. The fact that the synchrotron nebula has not broken free of the confinement of the filaments can best be understood if there is an extended remnant of freely expanding ejecta surrounding the Crab. The R-T unstable interface can be quantitatively understood as the cooling region behind a shock driven into this extended remnant by the pressure of the synchrotron nebula.

Key words: INSTABILITIES — ISM: INDIVIDUAL OBJECTS (CRAB NEBULA) — ISM: JETS AND OUTFLOWS — ISM: STRUCTURES — ISM: SUPERNOVA REMNANTS — SHOCK WAVES — STARS: PULSARS

1. INTRODUCTION

The *Hubble Space Telescope* is generally thought of as an edge-of-the-universe instrument, hence its name. However, since the installation in 1993 of the WFPC2, the *HST* has also proven itself a powerful tool for the study of the physics of nebulae. Even though nearby nebulae can be very large in the sky, they are shaped by physical processes occurring over the very short spatial scales associated with cooling lengths, radiative

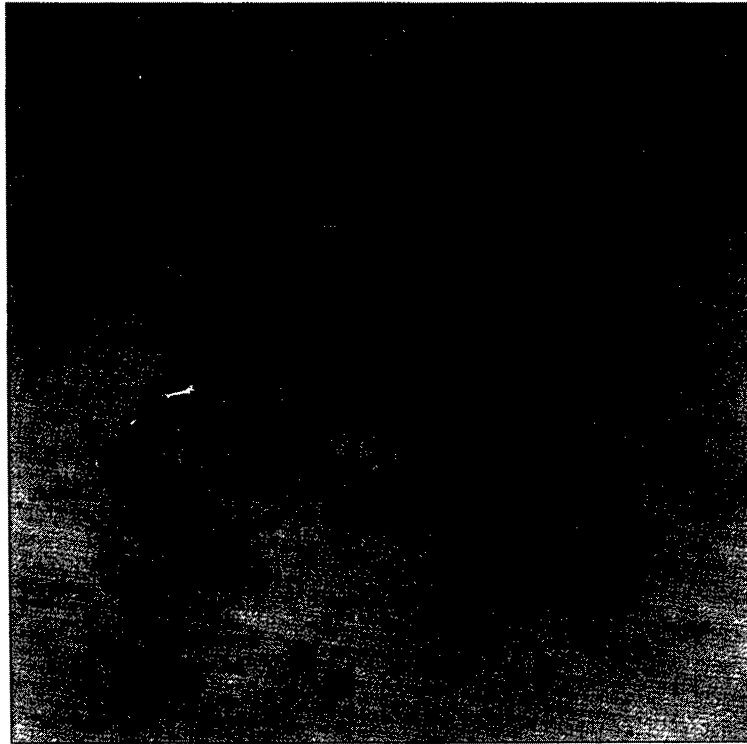


Fig. 1. Figure 8 from Hester et al. (1995), showing the structure of the inner part of the Crab synchrotron nebula visible in a 5500\AA continuum image taken with the *HST* WFPC2.

transfer, and the development of flow instabilities. The Crab Nebula has been no exception to this rule. The remnant of a supernova explosion witnessed by Chinese astronomers in 1054 AD, the Crab has been studied in every wavelength regime from radio through gamma rays, and probably has been observed using virtually every instrument capable of pointing at that part of the sky. In the outer part of the Crab is a complex of emission-line filaments composed of ejecta that was blasted into interstellar space by the supernova explosion. At the center of the Crab is the 33 ms Crab pulsar, which was the first pulsar to be observed at visible wavelengths. Connecting the two components is the Crab synchrotron nebula, which consists of relativistic particles and magnetic fields supplied by the wind from the pulsar. The pressure of the Crab synchrotron nebula is also responsible for pushing on and accelerating the expanding complex of filaments. *HST* observations are providing fascinating new insights and understandings, as well as raising new questions, about all of these components.

2. THE CRAB SYNCHROTRON NEBULA

WFPC2 observations of the Crab synchrotron nebula are presented by Hester et al. (1995; hereafter H95). These observations show an axisymmetrical structure in the synchrotron nebula, consistent with an axis of symmetry running from SE to NW and tipped into the plane of the sky by an angle of about 30° (see Figure 1). This is the same axis of symmetry inferred from observations of an X-ray torus in the Crab (Aschenbach & Brinkmann 1975). Fabry-Perot observations by Lawrence et al. (1995) also show that the filaments are concentrated in a band surrounding this same axis.

2.1. Sharp Structure in the Equatorial Torus

Small scale structures are seen throughout the Crab synchrotron nebula in the WFPC2 image. The sharpest of these in the main body of the nebula are localized to the region of the X-ray torus. Very thin striations with widths of only $0''.2$ or less can be traced around the entire circumference of the X-ray torus region. This region

is where some of Scargle's (1969) wisps were seen, including his wisp 2. Localization of these extremely sharp features to the region of the torus supports the association of the torus with a shock in the equatorial wind from the pulsar. Such a wind may be described by the striped magnetic wind solution of Coroniti (1990) or Michel (1994).

Such sharp striations cannot persist for long. Comparison of the scale of these structures with the sound speed in the relativistic synchrotron nebula gives time scales for their evolution of order a few days. To follow the temporal evolution of sharp structures in the Crab synchrotron nebula we used the *HST* to obtain a sequence of observations of the Crab over the course of the Crab's 1995-96 window of visibility. This series of observations included images taken as little as a week apart (Hester et al. 1996a). The time sequence observations show that the wisps in the Crab synchrotron nebula are moving outward through the region of the X-ray torus at speeds of about $0.5c$. This speed is much less than the velocity of the wind itself, so this must be shocked material. Figure 2 shows a sequence of these observations. The arrow indicates one especially bright wisp, which can be followed through the images over the course of about two and a half months. The wisp begins as a very diffuse structure that sharpens and brightens as it moves out, then fades into the background.

The evolution of this structure might best be understood as a cooling instability in the flow of shocked relativistic wind away from the pulsar. At the location where it shocks the pulsar wind must be dominated by particle energy rather than magnetic energy (Rees & Gunn 1974). This means that the plasma is far from the equipartition peak in the synchrotron emissivity. As a result, localized variations in the strength of the magnetic field will lead to variations in the strength of synchrotron emission. Regions which begin with stronger than average magnetic field will radiate more efficiently, losing pressure support and being compressed by the surrounding material. This further compresses the magnetic field, causing the region to brighten further. What began as a region of modestly stronger magnetic field becomes a sharpening region of progressively brighter synchrotron emission. This process should continue until equipartition is reached, at which point further compression no longer leads to dramatic increases in emission. Evolution of the surrounding region catches up with the wisp, and the wisp fades into the background. This outward moving material is decelerated as it pushes into the synchrotron nebula.

2.2. The Halo

Not all of the wisp-like structures in the Crab move outward in the manner described above. Two wisps, Scargle's "thin wisp," which is the wisp closest to the pulsar, and his wisp 1 remain stationary throughout the series of observations. Wisp 1 is concave toward the pulsar, like most wisps, but has a smaller radius of curvature than the wisps that move outward through the torus region. The thin wisp, on the other hand, is convex toward the pulsar, unlike all other wisps. Analysis of a sum of all of the data, including a ground-based image from van den Bergh & Pritchett (1989) seem to show that wisp 1 and the thin wisp actually close into each other, forming a "halo." The aspect ratio of the halo is very close to the aspect ratio of the X-ray torus. Assuming that the halo is actually circular, this indicates that it is inclined to the plane of the sky by the same amount, and surrounds the same axis of symmetry as the torus. The existence of this halo was proposed by H95. The plane of the halo is located about 1.4×10^{17} cm from the pulsar. Assuming that the axis of symmetry is an extension of the spin axis of the pulsar, the halo is located at a latitude of about 35° with respect to the pulsar. The cause of the halo remains unclear.

2.3. The Knot

Possibly the most surprising feature in the *HST* observations of the Crab synchrotron nebula is the presence of a bright knot located about $0.5'$ to the SE of the pulsar along the axis of symmetry of the nebula. The extended arc-like appearance of the knot in the original *HST* observations, as well as its location near the pulsar and along the axis of the nebula, suggest that it is a close-in feature in the high latitude wind from the pulsar (H95). Subsequent observations confirm this interpretation. The knot is highly polarized with a magnetic field running perpendicular to the axis of symmetry. It is also time-variable in its brightness and morphology, and moves in and out with respect to the pulsar by $0.1'$ or so. Stacking of all available *HST* data reveals the presence of no corresponding knot on the other side of the pulsar at a limit that is down by a factor of 60 from the SE knot. Due to the shallow tilt of the axis with respect to the plane of the sky this cannot be easily explained by Doppler beaming (H95). As a result, the knot seems to require a pronounced asymmetry in the structure of the pulsar wind. The physical nature of the knot is not understood.

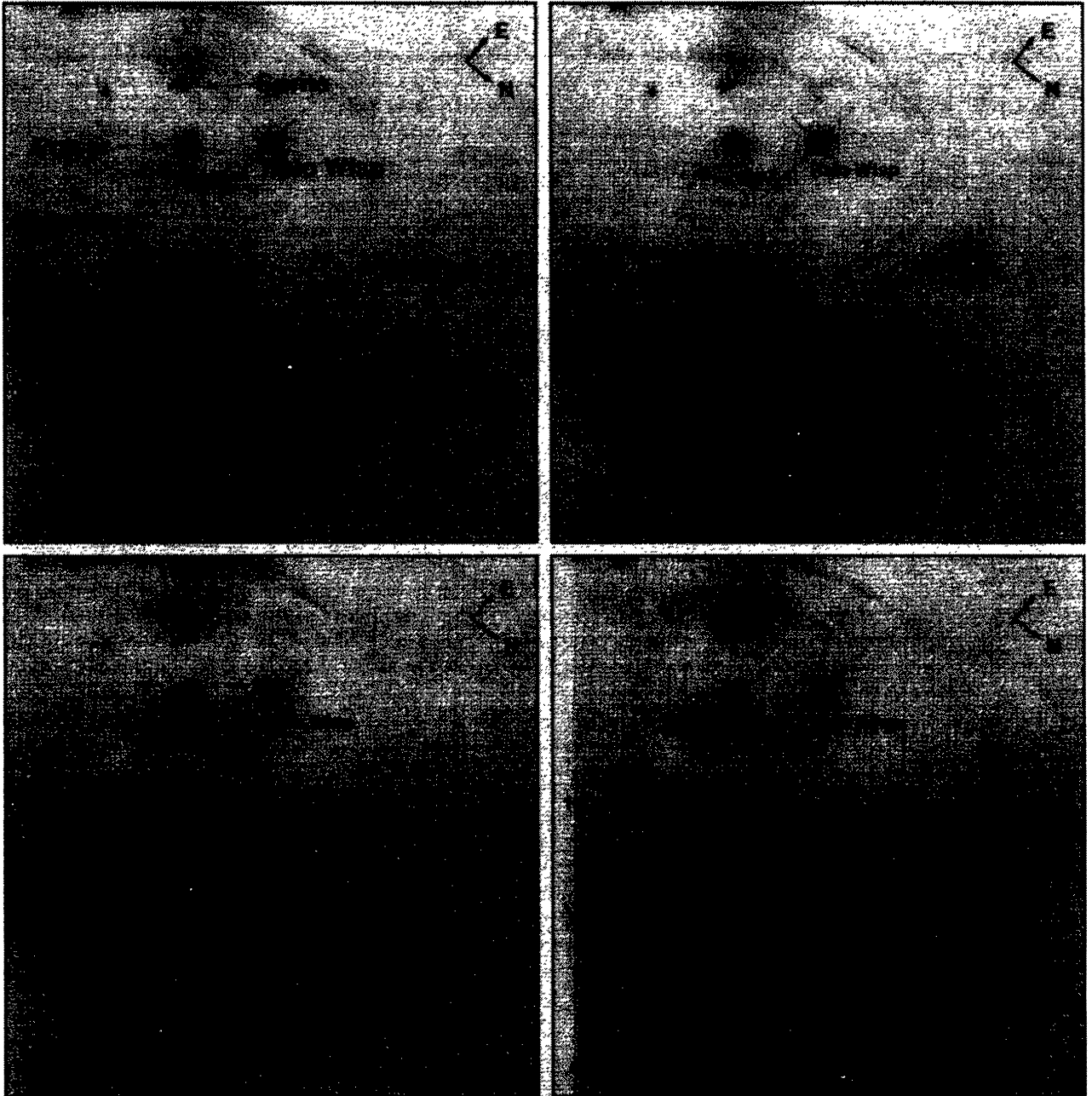


Fig. 2. Four images taken as part of a program to monitor the temporal evolution of the Crab with the *HST*. The arrows show the evolution of a wisp-like feature (“Feature A”) in the equatorial wind as it appears, brightens and steepens, then fades. This feature is moving away from the pulsar at about $0.5c$. Also note the persistence of the “halo” to the NW of the pulsar, and the highly dynamical nature of the “sprite.” These images are rotated with respect to Figure 1.

2.4. The Jet and Sprite

X-ray images of the Crab show a jet and a counter jet extending along the symmetry axis of the nebula. The more prominent of these structures, seen to the SE of the pulsar, can also be clearly identified in optical images of the Crab. In addition, the *HST* images of the Crab show striations which “drape over” the X-ray counter jet. These striations presumably trace the magnetic structure of the nebula, and their geometry suggests that the counter jet is “pushing into” the body of the synchrotron nebula. There is a knot of emission about 4'' to the SE of the pulsar, along the direction of the jet (Knot 2 in Figure 1). The time sequence of images show that this knot is the most dynamic feature in the nebula, changing its location and appearance dramatically between images separated by only six days. The dynamic character of this feature earned it the nickname of the “sprite.” Diffuse material can also be seen moving away from the pulsar off of the back side of the sprite at speeds of around $0.5c$. The sprite is interpreted as a shock in the polar jet from the pulsar.

Taken together, the *HST* images of the inner part of the Crab synchrotron nebula reveal a complex axisymmetrical structure ranging from an equatorial wind that shocks at distance of over 10^{18} cm from the pulsar, to strong polar jets containing features as close as 10^{16} cm from the pulsar. This complex structure is not symmetrical from one pole of the pulsar to the other. These observations provide the boundary conditions which must be matched by realistic models of the pulsar wind.

3. *HST* OBSERVATIONS OF THE CRAB FILAMENTS

Emission line observations of the Crab filaments show a range of ionization structures. The brightest filaments tend to have a stratified ionization structure with the lowest ionization emission from the interior of a filament and higher ionization emission surrounding the filament core. This can be seen in Figure 3. Extinction due to dust in the filament core can also often be seen against the background of the synchrotron nebula. This stratified ionization is as expected for a centrally condensed filament embedded within the radiation field of the synchrotron nebula. We have begun an effort to model the ionization structure of the Crab filaments (Sankrit & Hester 1998).

Perhaps the most remarkable aspect of the *HST* observations of the Crab filaments is that the filaments generally consist of radial fingers pointing into the interior of the nebula. These fingers are connected to their neighbors at their outermost points by narrow, faint, high ionization arcs. Hester et al. (1996b; hereafter H96) showed that this structure can be understood as the result of a Rayleigh-Taylor instability between the synchrotron nebula and swept-up ejecta. The linear theory for magnetic Rayleigh-Taylor instabilities was worked out over three decades ago by Chandrasekhar (1961), who balanced the buoyancy term driving the instability against the magnetic tension which stabilizes the instability. In the linear theory there is a relationship among the magnetic field, the wavelength of the instability, the effective gravity, and the density contrast across the interface. All four of these quantities are observable in the Crab. Observations of the Crab synchrotron nebula give a magnetic field of around 3–600 μG . Examination of the *HST* images gives a wavelength for the instability that is typically 1–3''. The acceleration at the edge of the Crab can be obtained from the fact that the filaments are expanding faster than the free expansion velocity (e.g., Trimble 1968), assuming an explosion date of 1054 AD. Values for the acceleration are around $3.5 \times 10^{-3} \text{ cm s}^{-2}$. The density of the material at the edge of the Crab can be estimated from its brightness in the *HST* images to be around 200–300 cm^{-3} . Observations of these four quantities satisfy the linear relationship for the onset of magnetic Rayleigh-Taylor instabilities, putting the argument based on morphology alone onto a strong physical footing.

The structure of the filaments can be compared with models of magnetic R-T instabilities by Jun, Normal, & Stone (1995). These models show that the strength of the magnetic field controls the nonlinear development of the instability. In the absence of a magnetic field, or for very weak magnetic fields, as the R-T instability develops dense material accelerates through the lighter material, and Kelvin-Helmholtz instabilities develop as a result of the velocity shear between the fluids. These secondary K-H instabilities are responsible for introducing vorticity in the fluid and for much of the mixing between the light and dense material. As the instability develops the dense fluid breaks into discrete clumps and strands which are surrounded by fluid at an intermediate density.

In the limit of very strong magnetic field, the field stabilizes the interface altogether. However, even if the field is not strong enough to prevent the onset of the R-T instability, as R-T fingers grow the magnetic field is drawn along the necks of those fingers and amplified. The field along the fingers may then be strong enough to prevent the development of secondary K-H instabilities. In this case, rather than vorticity, mixing, and clumping, the development of the R-T instability forms blunt fingers with well-defined edges and little mixing between the two fluids. Analogs of all of these filament types can be found within the Crab Nebula

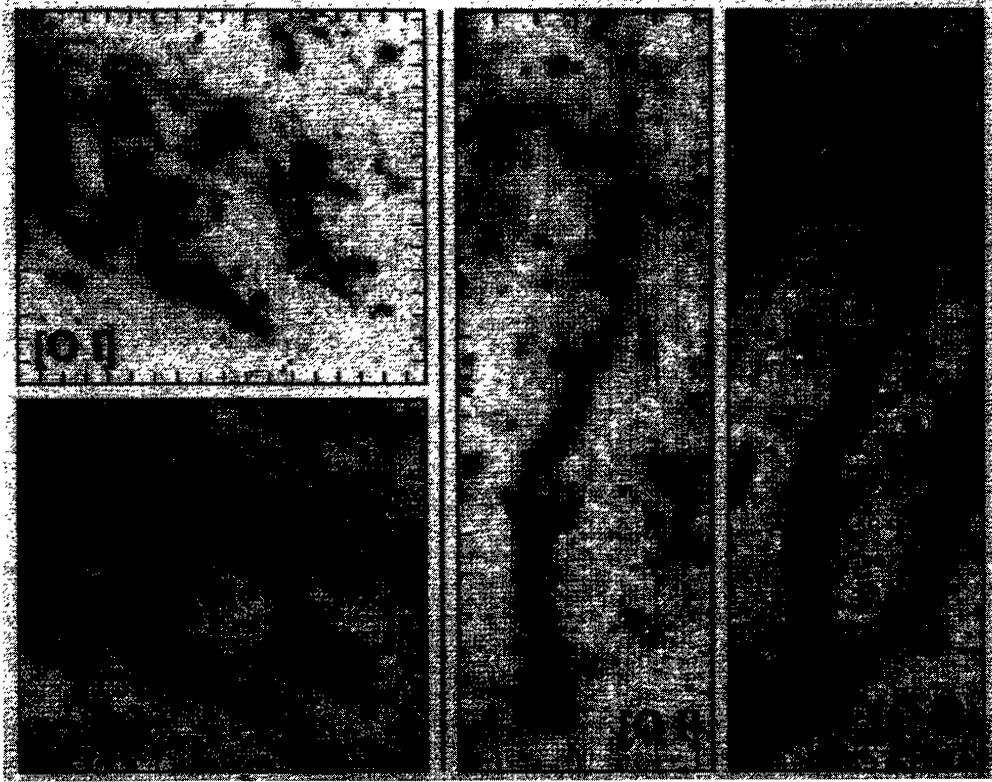


Fig. 3. [O I] $\lambda 6300$ and [O III] $\lambda 5007$ images of filaments in two fields in the Crab. Each tick mark is $1''$. (a) Filaments in which the magnetic field had very little effect on the development of R-T instabilities. (b) A R-T finger which has been partially stabilized by the magnetic field. Note the differences in morphology between the low and high ionization lines, and in particular the core-halo structure of the filament on the right.

(see Figure 3). H96 suggest that most of the filaments in the Crab can be understood as the result of a one-dimensional sequence with the key parameter being the relative strength of the buoyancy force and the magnetic field when the instability developed.

4. THE SHOCK AROUND THE CRAB

The R-T unstable interface itself can be seen in the *HST* images as the arcs connecting each R-T finger to its neighbors. In deep ground-based images this “skin” can be followed around most of the perimeter of the nebula (Figure 4a). The existence of this skin is something of a puzzle. The R-T instability is very efficient at removing material from the skin and concentrating it into filaments. In essence, the R-T instability serves the purpose of getting this material out of the way of the expanding synchrotron nebula. The continued existence of the skin really only makes sense if there is additional material beyond the visible boundary of the Crab, which continues to accumulate on the surface of the synchrotron nebula. In the absence of such surrounding material the synchrotron nebula should very quickly break through the filaments altogether. It was on the basis of this argument that H96 inferred the existence of an extended remnant of ejecta around the Crab.

In this view the “skin” seen in the ground-based and *HST* images is the cooling region behind a radiative shock which is driven into the extended freely expanding remnant by the pressure of the synchrotron nebula (Figure 4b). Sankrit & Hester (1997) consider the properties of such a shock. They find that the characteristics of the shock are determined by the physical properties of the nebula itself. The shock velocity is just the difference between the expansion velocity of the outer part of the nebula and the free expansion velocity at that radius assuming an explosion date of 1054 AD. Observations of the expansion of the Crab set this velocity between about 150 and 300 km s^{-1} . The pressure driving the shock is just the pressure of the synchrotron nebula. The density of the preshock medium is then established by momentum balance across the shock, setting $P = \frac{3}{4}\rho v^2$.

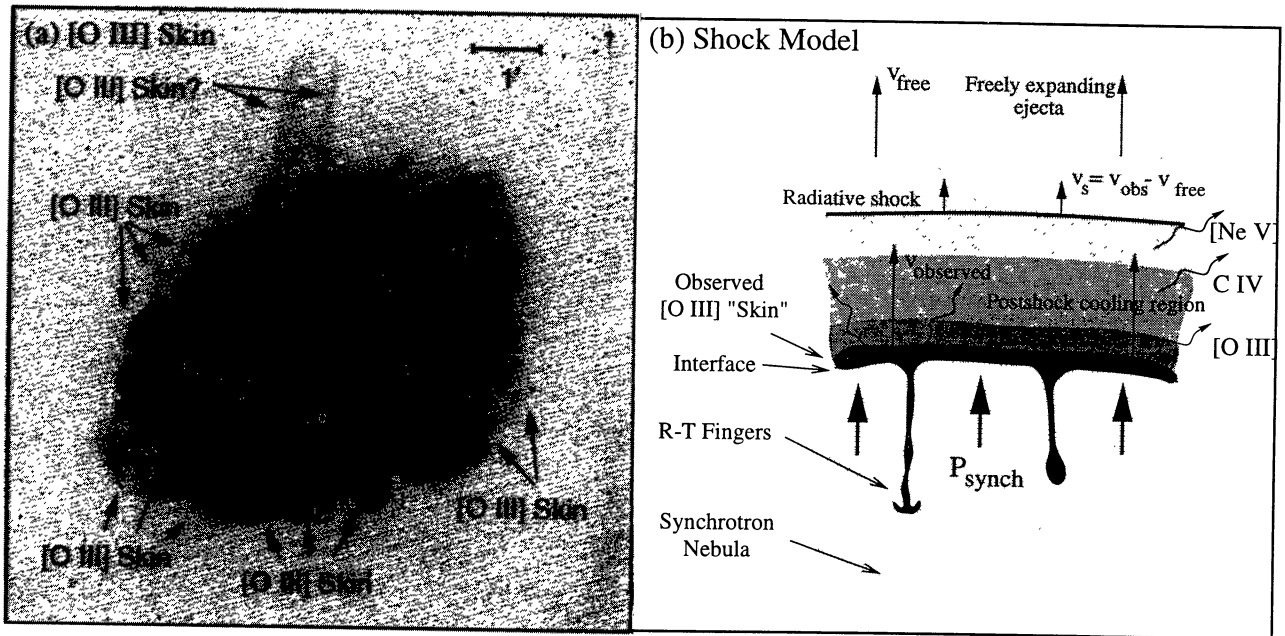


Fig. 4. (a) A deep ground-based [O III] image of the Crab taken with the 1.5-m telescope at Palomar Observatory. Note the existence of a “skin” of [O III] emission surrounding much of the Crab. This is the R-T unstable interface, which Sankrit & Hester (1997) interpret as the cooling region behind a shock being driven by the pressure of the synchrotron nebula into an extended remnant of freely expanding ejecta. The squares and numbers show $100 \times [\text{Ne V}]/[\text{O III}]$ from Davidson (1979). (b) A cartoon model of the structure of the interface.

Sankrit & Hester ran an isobaric sequence of shock models using the pressure of the Crab across the velocity range allowed by observations of the expansion of the nebula. They found that these models correctly predict the observed [O III] surface brightness of the Crab skin. While they were also able to match the [O III] emission from the skin using a photoionization model for material at the boundary of the Crab, the shock models and photoionization models differ markedly in their predictions for the strength of lines from high ionization potential species such as C IV and [Ne V]. A number of authors have been puzzled by the presence of such strong high ionization lines in spectra of the Crab. Blair et al. (1992) discuss a UV spectrum of the Crab obtained with the *Hopkins Ultraviolet Telescope*. They note the existence of a ubiquitous diffuse component of strong C IV seen on both the red- and blue-shifted sides of the remnant. Blair et al. identified this C IV emission with a smooth component seen in Fabry-Perot observations of the [O III] emission from the Crab. This is the same component which H96 identified with the R-T unstable interface and which Sankrit & Hester interpret as the cooling region behind the shock. Blair et al. attempted to explain the very high C IV/He II ratio in this medium as the result of photoionization with a very high ionization parameter. However, such models fail to account for the presence of lower ionization [O III] emission, and also require a thick region of emission in order to account for the brightness of the line. Sankrit & Hester, on the other hand, find that the C IV/He II ratio is just as predicted in their radiative shock models with velocities around 150 km s^{-1} .

Another observation of high ionization emission from the Crab is the detection of [Ne V] $\lambda 3426$ by Davidson (1979). As with the C IV observations, Davidson found the [Ne V] to be “remarkably strong” in comparison with expectation based on photoionization. Davidson also reported by far the strongest [Ne V] in several locations at the very boundary of the observed remnant. Reconstruction of his observations on our deep ground-based [O III] image of the Crab shows that these are spectra of the skin (Figure 4a). Shock models correctly predict the brightness of the [Ne V] emission for shock velocities greater than about 170 km s^{-1} .

To quickly summarize, the existence of a “skin” on the surface of the Crab synchrotron nebula only makes dynamical sense if there is an extended remnant surrounding the Crab and confining the synchrotron nebula. Having postulated the existence of such an extended remnant, the skin is then understood as the cooling region

behind a radiative shock driven by the pressure of the synchrotron nebula into this extended, freely expanding remnant. Models of this shock, which are tightly constrained by the physical properties of the Crab, correctly predict the properties of the skin, including its brightness in high ionization lines of C IV and [Ne V]. More "traditional" photoionization models of the skin fail in all of these respects. Sankrit & Hester (1997) conclude that taken together these observations demonstrate the existence of a shock and extended remnant around the Crab. The existence of a halo around the Crab has been a subject of great controversy for some time. Despite a number of claims, no direct observational evidence for such an extended remnant has been found (Fesen, Shull, & Hurford 1996). This is not surprising. Hester and Sankrit found that the extended remnant implied by the observed properties of the Crab could hold several solar masses of material and carry over 10^{50} ergs of kinetic energy and yet still remain invisible in deep observational searches.

5. CONCLUDING REMARKS

Even though the Crab Nebula is a relatively large object in the sky, and has been intensively studied in all wavelength regimes, much of the physics responsible for shaping the nebula occurs on spatial scales that are sharper than had been accessible in previous observational work. *HST* images of both the Crab synchrotron nebula and the ejecta from the explosion and the region of interaction between the two have significantly advanced our understanding of the nature of this enigmatic object.

The author would like to thank and acknowledge his collaborators in this work, including Paul Scowen and Ravi Sankrit at ASU, Curt Michel at Rice, Jay Gallagher at the University of Wisconsin–Madison, James Graham at UC Berkeley, and Alan Watson at New Mexico State University. Many of the observations presented here were taken as part of the science program of the Investigation Definition Team for the WFPC2, John Trauger, PI. This work was supported by NASA/JPL contracts 959289 and 959329.

REFERENCES

- Aschenbach, B., & Brinkmann, W. 1975, *A&A*, 41, 147
 Blair, W. P., Long, K. S., Vancura, O., Bowers, C. W., Conger, S., Davidsen, A. F., Kriss, G. A., & Henry, R. B. C. 1992, *ApJ*, 399, 611
 Chandrasekhar, S. 1961, *Hydrodynamic and Hydromagnetic Stability* (Oxford: Oxford Univ. Press)
 Coroniti, F. V. 1990, *ApJ*, 349, 538
 Davidson, K. 1979, *ApJ*, 228, 179
 Fesen, R. A., Shull, J. M., & Hurford, A. P. 1996, *AJ*, 113, 354
 Hester, J. J., Scowen, P. A., Sankrit, R., Michel, F. C., Graham, J. R., Watson, A., & J. Gallagher, 1996a, *BAAS*, 28, 950.
 Hester, J. J., et al. 1995, *ApJ*, 448, 240 (H95)
 Hester, J. J., et al. 1996b, *ApJ*, 456, 225 (H96)
 Jun, B.-I., Norman, M. L., & Stone, J. M. 1995, *ApJ*, 453, 332
 Lawrence, S. S., MacAlpine, G. M., Uomoto, A., Woodgate, B. E., Brown, L. W., Oliverson, R. J., Lowenthal, J. D., & Liu, C. 1995, *AJ*, 109, 2635
 Michel, F. C. 1994, *ApJ*, 432, 239
 Rees, M. J., & Gunn, G. E. 1974, *MNRAS*, 167, 1
 Sankrit, R. & Hester, J. J. 1997, *ApJ*, in press
 _____, 1998, *ApJ*, submitted
 Scargle, J. D. 1969, *ApJ*, 156, 401
 Trimble, V. L. 1968, *AJ*, 73, 535
 van den Bergh, S., & Pritchett, C. J. 1989, *ApJ*, 338, L69